

IBM Research Report

The Impact of Added Base on Imaging in a Positive Tone Chemically Amplified Photoresist

F. A. Houle, W. D. Hinsberg, M. I. Sanchez

IBM Research Division
Almaden Research Center
650 Harry Road
San Jose, CA 95120-6099



Research Division

Almaden - Austin - Beijing - Haifa - India - T. J. Watson - Tokyo - Zurich

The impact of added base on imaging in a positive tone chemically amplified photoresist

F. A. Houle, W. D. Hinsberg and M. I. Sanchez
IBM Almaden Research Center, 650 Harry Road, San Jose, CA 95120

Abstract

The inclusion of base in chemically amplified resist formulations is known to improve imaging, yet the mechanism by which this occurs, and the effect of different chemical types of base is poorly understood. Previously we showed that tetrabutylammonium hydroxide (TBAH), an ionic base, added to *p-tert*-butyloxycarbonyloxystyrene (PTBOCST) - *t*-butyl iodonium perfluorobutane sulfonate (TBI-PFBS) positive tone chemically amplified resist affects local acid concentrations in exposed photoresist through a pre-neutralization mechanism. We have now extended these studies to include a neutral base, 7-diethylamino-4-methylcoumarin (7DEAMC), and show that it operates by a qualitatively different process. Using the rate coefficients obtained for both bases, we investigate the impact of the details of the neutralization kinetics on image formation in PTBOCST/TBI-PFBS resist as a function of pitch and dose. The results show that the selection of base can be expected to play an important and complex role in the evolution of the acid and deprotected resist images during post-exposure bake. A framework for understanding the role of base is proposed.

Introduction

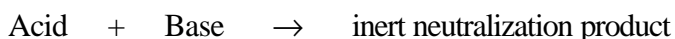
The addition of small quantities of basic compounds to chemically amplified (CA) resist formulations have been reported to lead to longer shelf-life, increased image resistance to airborne chemical contamination and substrate contamination effects, and to impart improved lithographic imaging properties.¹⁻⁶ Typical additives include n-methyl pyrrolidone, polymeric and nonpolymeric amines, and ionic hydroxide salts, in both photolabile and photoinert forms. The role of base has generally been described as acting as a trap for acid that diffuses from the exposed into the unexposed area.

In a very simple picture, added base can be thought of as playing two distinct but interrelated roles. They are illustrated in Figure 1, which shows a schematic diagram of concentration profiles of photogenerated acid and base during CA resist processing. Typically, high-resolution imaging using projection lithography produces a latent image of photogenerated acid in the resist where even the nominally unexposed areas contain a small quantity of acid, a consequence of the diffraction of light (Figure 1(a)). The effect of this “background” acid is to cause deprotection in the nominally unexposed regions of the film, which leads to image blur. (In this work, image blur is defined to be a general broadening of a latent image during resist processing due to chemistry and diffusion.) If an added base reacts with the photogenerated acid at a rate that is competitive with or faster than acid-catalyzed deprotection, then the base can be thought of as effectively scavenging this background acid (Figure 1(b)). While the rate of deprotection is slowed overall because of the reduction in acid catalyst concentration, the rate suppression in nominally unexposed regions is proportionately more, in the limit being completely suppressed if the amount of base exceeds the amount of acid. The net effect is that the

contrast of the image, that is, the difference in extent of deprotection in the exposed and unexposed regions, is increased.

This first role is independent of the specific diffusion characteristics of the acid outside of the local mobility required for the neutralization reaction to occur, and is operative even in the absence of long-range acid diffusion. There is a second, diffusion-related role as well. If the amount of base added exceeds the amount of acid generated in the unexposed areas during exposure, then there is a residual amount of base in those regions (Figure 1(c)). If acid diffuses into the unexposed regions then it will encounter base and will undergo neutralization if the kinetics allow, suppressing the acid catalyzed deprotection that is a chemical consequence of acid diffusion. This process serves to reduce image blur.

Basic additives are selected for particular resist formulations using a variety of criteria, yet there is little systematic, fundamental understanding of how various base types work in the resist, and even more importantly, what impact the chemistry of a particular base will have on the latent and developed images formed in the resist. Moreover, it is not even known whether the model presented in Figure 1 is actually correct. The foundation laid in our earlier work on the chemistry and physics of the post-exposure bake (PEB) process is a reaction-diffusion model that describes quantitatively the competition between acid diffusion and acid-catalyzed deprotection.⁷⁻¹⁰ The 4-step chemical mechanism is readily extended to include an acid-base neutralization step during PEB:



The instantaneous overall rate R_n of the neutralization reaction in each area of the film is assumed to be described by the rate law $R_n = k_n [A][B]$, where k_n is the rate constant for neutralization at a given temperature, and $[A]$ and $[B]$ are the instantaneous local concentrations of acid and base, respectively. The constant k_n should be considered a composite value; overall the neutralization reaction includes interaction of the species with the polymeric matrix and rearrangement of the matrix to facilitate site hopping of the reactants, so the rate constant will reflect some combination of these processes. Although it is generally presumed that base diffuses during PEB,⁶ we have neglected this process as a first approximation.

Using this approach as a starting point, we have begun to investigate the role of base in positive-tone chemically amplified photoresists. In a preliminary report we described the chemistry of an ionic base, *tert*-butyl ammonium hydroxide (TBAH) and identified its neutralization mechanism.⁷ Subsequently, we showed that the kinetics also applied to imaging a line-space array pattern.⁹ In this paper, we extend this work to compare the behavior of TBAH to that of an amine, and use our experimentally validated reaction-diffusion model to explore the impact of the two types of bases on image formation as a function of pitch and dose. The results show that the picture described above is too simple: there is significant subtlety to the interaction between base, acid and polymer during post-exposure bake that must be properly captured for accurate prediction of resist images.

Experimental

We have developed a two-step experimental - simulation approach to characterize the kinetics of latent image transformation during PEB.^{7,8} Briefly, the detailed deprotection chemistry is first studied

under conditions where the resist film is uniformly exposed, leading to a quantitative description of the chemical kinetics of the system that is accurate over a wide range of temperatures, acid concentrations and resist compositions. Then, the experiment is repeated under conditions where a thin 200 nm thick layer of exposed resist containing acid is formed at the surface of a much thicker 1000 nm unexposed layer. This is achieved by irradiating a 1200 nm thick resist film with a 193 nm UV source, a wavelength where the film is very strongly absorbing. Since the overall extent of deprotection in the film is readily quantified by monitoring the intensity of a characteristic TBOCST absorption in the infrared spectral region, and the chemical deprotection kinetics are known, the acid diffusion kinetics can be extracted from the data using reaction-diffusion modeling. The 1-dimensional kinetics thus obtained have been shown to describe line-space array formation, indicating that the mechanism is not lacking any features important for describing patterning on length scales as small as 50 nm at this stage.⁹

This approach has been applied to studies of the kinetics of resists containing base. In addition to verifying the deprotection kinetics, blanket exposed films were used to check that the equivalency of each concentration of base added to each formulation was correct by comparing measured and simulated deprotection curves.

Materials. The CA resist formulations we have examined in this study are based on the poly(*tert*-butoxycarbonyloxy)-styrene) (PTBOCST) polymer, one of the simplest and best-characterized CA resist polymers. We have examined resist formulations where PTBOCST is combined with the photoacid generator (PAG) di-(*tert*-butylphenyl)iodonium perfluorobutanesulfonate (TBI-PFBS), which generates perfluorobutanesulfonic acid (PFBS-A) upon irradiation. Resist solutions

were prepared in propylene glycol methyl ether acetate solvent containing PTBOCST and sufficient PAG to yield a loading of 0.045 moles/kg solids in the coated film. Resist solutions containing added base were prepared by including in the liquid mixture an amount of tetra-*n*-butylammonium hydroxide (TBAH) sufficient to yield TBAH concentrations in the films that ranged from 0.009-0.045 moles/kg solids (0.2-1.0 equivalents relative to the amount of PAG). Although the ionic base initially added to the resist solution is pure TBAH, there is evidence from other work¹¹ that it undergoes rapid reaction and is unlikely to be the sole basic species in the film. Reaction of OH⁻ with solvent to generate lactate anion, or with polymer to generate phenolate anion are likely to occur. The specific chemical identity of the ionic base is not important for the model discussed here. The amine chosen was 7-diethylamino-4-methylcoumarin (7DEAMC), added in similar concentrations. This amine is involatile, and therefore its concentration is expected to remain stable during processing of the wafers.

Film preparation and spectroscopy Films were prepared at a thickness of 1200 nm by spin-coating directly onto silicon wafers precoated with BARL 900 antireflection coating for those films exposed to 254 nm light, and were post-apply baked at 130 °C for 90 sec prior to exposure. Wafers were exposed to doses of 75 mJ/cm² at 193 nm for the 1-dimensional reaction-diffusion measurements, and 200 mJ/cm² at 254 nm to check base equivalencies. PEB was carried out in a Nicolet Continuum infrared microscope attached to a Nicolet Nexus 470 Fourier transform infrared spectrometer, or a Nicolet IR/44 Fourier transform infrared spectrometer. Both microscopes had heated stages held at 65 and 85 °C in order to measure film composition as a function of time.

Simulations

Two qualitatively different descriptions of acid - base neutralization occurring during PEB can be imagined. In the first model, *competitive neutralization* (CN), a fast acid-base reaction occurs in competition with acid-catalyzed deprotection. After coating, the PAG and base are present at a concentration that is uniform with depth in the film. During PEB, the photogenerated acid and the base react, leading to a progressive depletion of both acid and base in the exposed regions.

In the second model, *proportional neutralization* (PN) the added base is assumed to cause an initial proportional reduction in the amount of acid available after photolysis. As illustrated in Figure 2, during exposure the PAG undergoes photolysis with normal efficiency, but in this instance the presence of the base causes an overall reduction in the amount of acid formed, yielding an initial acid profile whose magnitude is reduced in proportion to the amount of base added. For example, if 0.2 equivalents of base were added to the formulation, then the acid at the start of the PEB step is scaled by a factor of $(1 - 0.2) = 0.8$, so that only 80% of the acid is available in each layer compared to the base-free formulation. Although the mechanism by which this occurs is unknown, the system behaves as if there is a type of pre-association between PAG and base that alters the acid-generating chemistry. The acid and base that remain following this proportional neutralization can then undergo a further competitive neutralization reaction during PEB. This is consistent with the work of Asakawa et al.² who have reported evidence for an initial partial capture of acid by added base at the very beginning of the PEB step, followed by further base-induced deactivation of the acid during the course of PEB.

To illustrate the impact of these two models on the deprotection kinetics as a function of base concentration, generic 1-dimensional reaction-diffusion simulations were carried out for these two

models at constant dose and PEB temperature (65 °C) using the activation parameters for deprotection and acid diffusion determined for the base-free formulation, and assuming an extremely fast neutralization rate.⁷⁻¹⁰ Film thicknesses were assumed to be 1200 nm. Figure 3 compares their predictions. A comparison of Figures 3a and b shows that the different assumptions in these models predict readily distinguishable behaviors as the base concentration added to the resist is increased.¹²

As will be presented in the Results section, experimental deprotection curves for TBAH and amine formulations were readily classified as best matching one of the two models. Simulations of the PEB process using the appropriate neutralization model were performed for each resist formulation as described in detail elsewhere^{7,8} in order to fit the value of k_n for two temperatures, 65 and 85 °C. Although it is generally presumed that base can diffuse,⁶ this was not initially included in the simulations because it would introduce an additional unknown into the model and reduce the likelihood that the extracted rate coefficients would be extendable. Our strategy in developing reaction-diffusion models is to work with the simplest description possible until that description fails. Accordingly, we worked to fit the experimental data obtained in this work using a single unknown - the neutralization rate constant - and were prepared to add base diffusion only if the fits were poor.

Once the kinetics for each resist were determined, additional simulations of line-space patterns were carried out to assess the impact of each base on the latent image formed during PEB. Three sets of calculations using 1200 nm thick films were done: (1) resists containing either of the two bases, and the base-free formulation at constant 8 mJ/cm² dose to compare the effect of pitch, 500 nm and 192 nm, (2) all formulations at a constant pitch, 192 nm, to compare the effect of dose (1 mJ/cm² and 8 mJ/cm²),

and (3) amine at 10 mJ/cm² dose to compare profiles using no base, TBAH and amine for similar extents of deprotection.

Results

Resist with ionic TBAH base. The deprotection curves for PTBOCST/TBI-PFBS resist with varying amounts of TBAH obtained at 65 C are shown in Figure 4a. By comparing them to Figure 3, it is evident that they most closely resemble the pattern found for PN kinetics (Figure 3b), not CN. The data in Figure 4 are overlaid with best fit PN simulations. The only adjustable parameter in the model is the value for k_n , the rate constant for acid-base neutralization, which is constant at a given temperature and cannot vary with base concentration. At 65 C a value of 2.5×10^{-3} l/mole-sec was obtained for k_n . Figure 4(b) shows experimental data obtained at 85 C, again overlaid with predictions of the PN model. At this temperature, a best fit was obtained when $k_n = 7.0 \times 10^{-2}$ l/mole-sec. Based on these two rate constants, an estimate of the activation energy for the overall neutralization is 40 kcal/mole. Assuming that the acid-base reaction is diffusion-controlled, k_n implicitly includes short-range acid and base motions as well as entropic contributions.

In solution the activation barriers for acid-base neutralizations are typically very small and such reactions occur upon essentially every encounter of the reactants. It is useful to compare the value of k_n derived here from experiment with that expected on theoretical grounds for such a diffusion-controlled reaction. A modified form of the Smoluchowski relation¹³ can provide an approximate value for the limiting rate constant $k_{n,diff}$ expected for acid-base neutralization at the diffusion-controlled rate in the partly deprotected PTBOCST matrix:

$$k_{n,diff} = \frac{4pr'N}{1000} (D_1 + D_2)$$

where r' is the sum of the radii of the reacting groups (in cm), N is Avogadro's number, and D_1 and D_2 are the diffusion coefficients of the two reactants in cm^2/sec . For this rough estimate we take the diffusion coefficient of base to be negligible (~ 0), the diffusion coefficient of HO-PFBS acid to be the average of the diffusion coefficient values in PTBOCST and in PHOST (the PTBOCST deprotection product) matrices at a given temperature⁸ and use a value of 4×10^{-8} cm (the sum of the sizes of the PFBS anion and tetrabutylammonium cation derived from molecular mechanics calculations¹⁴) as an estimate for r' . Using these values, $k_{n,diff}$ is estimated to be 0.08 l/mole-sec at 65 C, and 1.5 l/mole-sec at 75 C. The observed values of 0.0025 and 0.07 l/mole-sec are more than an order of magnitude less than these theoretical limiting values. In other polymer systems such departures from the limiting values have been attributed to entropic factors that serve to decrease the efficiency of bimolecular reaction, for example where only certain reactant orientations can successfully lead to reaction.¹³

The PN model provides an accurate quantitative description of the effect of base on deprotection in these experiments. As it must, the PN model also correctly predicts the effect of added base on deprotection kinetics for TBI-PFBS/PTBOCST films uniformly exposed using 254 nm light (data not shown). Explicit inclusion of base diffusion to achieve a good fit was not required, evidence that it is not kinetically significant for the reaction conditions investigated here.

Resist with neutral amine base. Data for deprotection of resist containing the amine at 65 and 85 C are shown in Figure 5. It is evident that the reproducibility of the data are poor, although since the extents of reaction are smaller than the corresponding data for TBAH the error is not unexpected. We found significant variations between aged and new solutions, particularly at large base concentrations, the aged solutions tended to show the smallest suppression of deprotection. Despite the scatter, it is evident on comparison with Figures 3 and 4 that the overall pattern of the curves is consistent with the CN model. Best fits are shown in the Figure. No attempt was made to fit the shape of the deprotection curves precisely because of the lack of reproducibility. The best fit rate constants for neutralization are 0.5 l/mole-s at 65 C and 3 l/mol-s at 85 C. Using the same assumptions made when applying the Smoluchowski relation to the TBAH compositions (see above), the values of k_n are on the order of those expected for diffusion controlled reaction, where essentially every encounter leads to neutralization. The uncertainty in the k_n is approximately a factor of 2, and an activation energy cannot be reliably drawn from these numbers. Although it is a possibility that the amine diffuses during the reaction, the data are not of sufficient quality to say definitively whether this is the case. The amine is bulky and diffusion rates are likely to be very small,⁸ so neglect of its diffusion is not a serious deficiency in the model.

Simulations of 192 nm pitch line-space arrays. In previous work⁸ investigating image blurring of line-space arrays as a function of resist formulation, the 85C PEB kinetics obtained for PTBOCST/TBI-PFBS/0.05equivalents TBAH resist using 193nm illumination in a 1-dimensional geometry were shown experimentally to be also valid for 192 nm pitch patterns over a dose range of 1-8 mJ/cm² using 257 nm light. Assuming that the amine kinetics are similarly valid, we carried out a

series of simulations at constant dose, temperature and base loading to investigate the impact of choice of base on the resist image. Maps of acid and deprotected PTBOCST images using a dose of 8 mJ/cm² as a function of time during PEB are shown in Figure 6. Although the initial acid concentrations are nearly the same, it is evident that the differences in the neutralization rates have a marked impact on the evolution of the latent images. The acid image in the amine resist fades quickly while the corresponding image in the TBAH resist does not. The deprotected polymer images reflect the degree of neutralization in each case: the extents of reaction decrease in the order no base > TBAH > amine.

To facilitate comparisons of results of different printing conditions, we have converted the maps into line plots of component amounts as a function of position across the resist line by averaging composition through the 1200 nm resist film thickness. Plots of acid at 0 and 5 min, and of HOST at 5 min derived from the data in Figure 6 are presented in Figure 7. It is clear that only the amine inhibits acid and polymer image blur. In fact, the TBAH acid image blurs out more than the base - free resist (PTBOCST/TBI-PFBS). Although full width half maximum of features printed with TBAH are the same as those with no base, the addition of TBAH results in a narrowing of the resist image at the edges of the exposed areas (near the acid minima), i.e. an improvement in contrast. The contrast of the amine and base-free formulations is similar. Very different results are found at 1 mJ/cm² dose, as shown in Figure 8. At the lower dose there is no contrast improvement conferred by using TBAH, indeed the base appears to affect the resist image only minimally. In contrast, the amine induces substantial line narrowing.

To assess the impact of base type on the shape of developable latent image in the resist under conditions of constant extent of reaction, a simulation using a dose of 10 mJ/cm² was carried out for the amine. Results are shown in Figure 9. Again, addition of the amine results in both acid and polymer image narrowing relative to the no base case, even though the dose is higher. The TBAH profiles are broader except at the edges of the exposed region. It is interesting to note that very similar developable profiles are formed despite the marked differences in the initial and final acid images as a result of the interplay between reaction and diffusion kinetics during post-exposure bake.

The trends in images as a function of dose and base can be understood by inspection of the simulated profiles comparing acid, base and HOST for each type of base in Figure 10. If base is initially absent in the areas of greatest acid concentration, as is the case for TBAH at high dose, blurring of the acid image is substantial. Some spreading is even seen at low dose, where the base concentration is simply depleted initially. The HOST image contrast is enhanced for TBAH at high dose, but unaffected otherwise. The amine, on the other hand, effectively eliminates acid blur at all doses by efficiently reducing the acid concentration. This causes an overall reduction in the amount of PTBOCST deprotection at both doses relative to that obtained with TBAH.

Simulations of 500 nm pitch line-space arrays. A set of calculations parallel to those for 192 nm was performed at 500 nm pitch, 8 mJ/cm², to assess the connection between feature size and impact of base on latent image. Maps of acid and deprotected PTBOCST images are shown in Figure 11. There are notable differences in the trends seen compared to those at smaller pitch. The acid latent image blur is minimal, and the reduction in local acid concentration with time is appreciable only for the amine. The

deprotected polymer images show a slight narrowing of the image with TBAH, and a substantial reduction in extent of reaction with amine. Line plots derived from the maps are shown in Figures 12 and 13. Unlike the 192 nm case, at 500 nm addition of TBAH results in a small improvement in resist image contrast. The presence of amine, on the other hand, does not affect contrast, and is less effective at inhibiting reaction than at 192 nm.

Discussion

The rationale for addition of base to improve resist images rests on an assumption that base acts to trap diffusing acid, thus narrowing the developable image formed in the resist. Within this scenario, all bases are equivalent, excepting cases where there are specific base-polymer interactions. The present work shows clearly that this simple picture does not capture the effect of base on resist image at all. The two types of base investigated here, ionic and neutral small molecules, obey qualitatively different kinetics, resulting in qualitatively different resist images for the same formulation and processing conditions. The differences are rather subtle at large pitch (500 nm) and substantial at small pitch (192 nm). The trends at small pitch are affected by dose: the images obtained using TBAH and amine are more similar at low dose than at high dose. Although the neutralization rate constant differs by a factor of forty for the two bases, the trends with dose signal that it is not the magnitude of the rate constant alone that dominates image formation: other aspects of the kinetics play important roles.

Figures 6, 9, 11 and 13 provide insight to a primary difference between the various cases explored in this work that may play a significant role in determining the resist image: the initial base distribution. At a dose of 8 mJ/cm^2 , TBAH is completely depleted in the strongly illuminated regions and present at full

concentration in unilluminated areas, while the amine has a uniform initial distribution. Consequently, the amine neutralization rate is much faster in illuminated than unilluminated areas, and competes effectively with deprotection and acid diffusion. It is interesting to note that at 192 nm pitch the spreading of the acid latent image is much less in the presence of amine than TBAH or no base. This is because the neutralization of the acid is more efficient, thus reducing its local gradient and the overall diffusion rate. This effect is less pronounced at 500 nm pitch since the initial spatial gradients are smaller. At a dose of 1 mJ/cm², TBAH is not completely depleted, and its impact on the resist image is similar to that of the amine. We can conclude that *the variations in the resist images with formulation, pitch and dose are therefore attributable to variations of the initial base distribution and the length scale of concentration gradients.*

The experiments and simulations reported here provide a framework for thinking about the impact of selection of base for a given resist that supercedes the simpler picture presented in Figure 1. That scheme carries an underlying assumption that the spatial characteristics of the resist image resulting from post-exposure bake correspond directly to the acid image.¹⁵ Inspection of Figures 6 - 13 shows that while this may be approximately true at large pitch (250 nm lines and spaces) it is not at all the case at small pitch (96 nm lines and spaces). An alternative model, shown in Figure 14, connects the final resist image to base function. We distinguish two limiting cases: case 1, in which base is initially absent in strongly illuminated areas but present elsewhere, forming a latent image that is the reverse of the acid image, and case 2, in which base is initially uniform everywhere. Case 1 primarily applies to TBAH and similar bases that interact strongly with the photoacid generator in the resist. In case 1, base does not slow the acid diffusion rate, it may even accelerate it somewhat because preneutralization serves to

steepen the initial acid gradients. Rather, its substantial concentration in unilluminated areas serves as a diffusion barrier to acid. The result is some contrast improvement, but little reduction in the spatial extent of the latent resist image because acid concentrations remain high. Case 2 applies to any base in concentrations sufficiently high that exposure does not cause complete depletion through preneutralization. The reaction rate between acid and base is fast enough to compete effectively with deprotection and acid diffusion, leading to notable sharpening of the resist image. In both cases, the detailed resist latent image shape (and hence image contrast) will depend on pitch, because the contribution of acid diffusion to image blur becomes more significant as feature sizes shrink. These contrast variations may result in changes in line-edge roughness with resist formulation, pattern dimension, and processing conditions.

It should not be inferred that process conditions for imaging will be the same for both cases - clearly competitive neutralization inhibits latent image formation, and an increase in sensitivity, dose or temperature would be needed to obtain sufficient deprotection for a pattern to develop through the full resist thickness. Other factors are also likely to be important. Evaporation of base during post-exposure will result in a continuous reduction in its concentration and dynamically reduce the neutralization rate. Base diffusion is neglected in this work because there is no evidence from the reaction - diffusion simulations that it is kinetically significant for the materials systems examined here. This may not be true for other bases and polymers since any gradient can lead to diffusion. The influence of the base diffusion rate on the deprotection kinetics should be evaluated for each case.

Conclusions

The effect of added TBAH and 7-diethylamino-4-methylcoumarin on post-exposure deprotection has been investigated experimentally in the TBI-PFBS/PTBOCST system, and is shown to be quantitatively describable with simple chemical models. The ionic base, TBAH, initially neutralizes a portion of the photogenerated acid presumably through a close interaction with the photoacid generator, and induces further competitive neutralization during PEB. The neutral amine, on the other hand, only participates in competitive neutralization. The differences in the kinetics play a crucial role in formation of the latent resist image, which is explored through experimentally-validated simulations of PEB as a function of resist composition, pitch and dose. We find that simple concepts such as line narrowing through acid trapping do not fully describe the role of base, and that blur in the acid image is not necessarily reflected in the resist latent image. The trends in acid and resist latent images can be understood using a framework that considers the spatial distribution of base to be of central importance to the final image characteristics. Capturing the subtle variations in resist latent image requires that the kinetics of deprotection, acid neutralization and acid diffusion be treated at a high level, particularly as feature size drops below 100 nm. More simplified treatments such as parameterized transformation of the initial aerial image are unlikely to be successful.

Acknowledgments

We are grateful to Greg Wallraff and Hiroshi Ito for useful discussions throughout the course of this work, and for providing unpublished data.

References

1. Y. Kawai, A. Otaka, A. Tanaka and T. Matsuda, *Jpn. J. Appl. Phys.*, **33**, 7023 (1994).
2. K. Asakawa, T. Oshirogouchi and M. Nakase, *SPIE Advances in Resist Technology and Processing XII*, **2438**, 563 (1995).
3. W. Huang, *SPIE Advances in Resist Technology and Processing XVI*, **3678**, 1040 (1999).
4. S. Funato, N. Kawasaki, Y. Kinoshita, S. Masuda, H. Okazaki, M. Padmanaban, T. Yamamoto and G. Pawlowski, *SPIE Advances in Resist Technology and Processing XIII*, **2724**, 186 (1996).
5. L. Ferreira, S. Malik, T. R. Sarrubi, A. J. Blakeney and B. Maxwell, *SPIE Advances in Resist Technology and Processing XV*, **3333**, 236 (1998).
6. H. Fukuda, K. Hattori and T. Hagiwara, *SPIE Optical Microlithography XIV*, **4346**, 319 (2001).
7. W. D. Hinsberg, F. A. Houle, M. I. Sanchez, M. E. Morrison, G. M. Wallraff, C. E. Larson, J. A. Hoffnagle, P. J. Brock, G. Breyta, *Proc. SPIE, Advances in Resist Technology and Processing XVII*, **3999**, 148 (2000).
8. F. A. Houle, W. D. Hinsberg, M. Morrison, M. I. Sanchez, G. Wallraff, C. Larson, and J. Hoffnagle, *J. Vac. Sci. Technol. B*, **18**, 1874-1885 (2000).
9. F. A. Houle, W. D. Hinsberg, M. I. Sanchez and J. A. Hoffnagle, *J. Vac. Sci. Technol. B*, in press (2002).
10. G. Wallraff, J. Hutchinson, W. Hinsberg, F. Houle, P. Seidel, R. Johnson and W. Oldham, *J. Vac. Sci. Technol. B*, **12**, 3857 (1994).
11. H. Ito, unpublished; J. W. Thackeray, M. A. Braintree, P. R. Hagerty, US 5,879,856, March 9, 1999.

12. Additional models for base neutralization kinetics including metathesis and formation of a photodecomposable base were explored in ref 7, and found to not match experiment.
13. M. Heskins and J. Guillet, *Macromolecules*, **3**, 224 (1970)
14. G. M. Wallraff, unpublished.
15. M. D. Smith and C. A. Mack, *Proc. SPIE, Advances in Resist Technology and Processing XVIII*, **4345**, 148 (2000), and references therein.

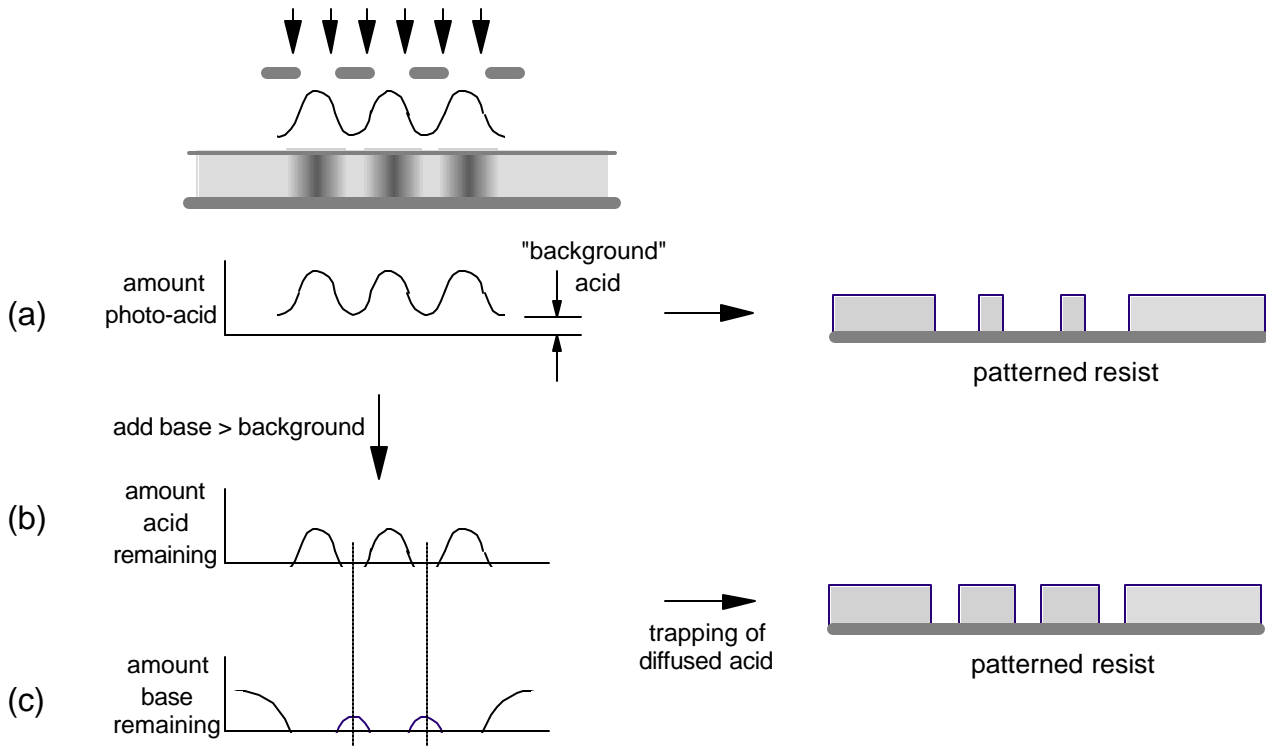


Figure 1. Qualitative depiction of the role added base is believed to play during post-exposure bake of a chemically amplified resist. (a) Exposure of a resist with no base results in formation of an acid latent image which would form a distorted pattern in the resist due to formation of small amounts of acid in nominally unilluminated areas. (b) Addition of base causes acid to be rapidly neutralized, leading to a more localized acid image. (c) Residual base is present in unilluminated areas in the resist, where it can act as a trap for diffusing acid. The result of (b) and (c) is a sharper resist image.

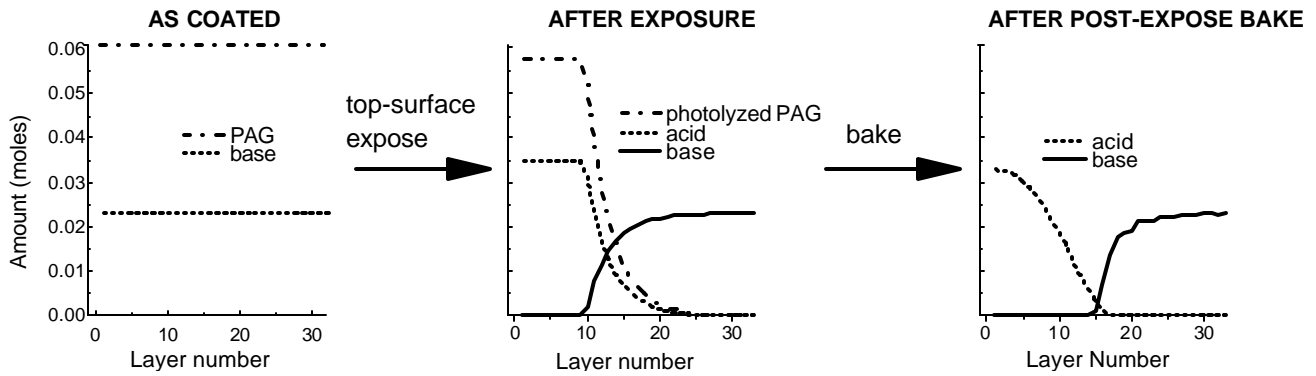


Figure 2. Schematic of the proportional neutralization model applied to the top-surface exposure geometry used to determine post-exposure bake reaction-diffusion kinetics. A resist film containing uniformly distributed photoacid generator and base is coated onto a wafer. After exposure to 193 nm light, which is strongly absorbed, the photoacid generator is completely decomposed. The acid initially formed is reduced in proportion to the base concentration present, resulting in complete depletion of base in the illuminated top region of film. The remaining base can neutralize acid diffusing under the influence of its steep concentration gradient.

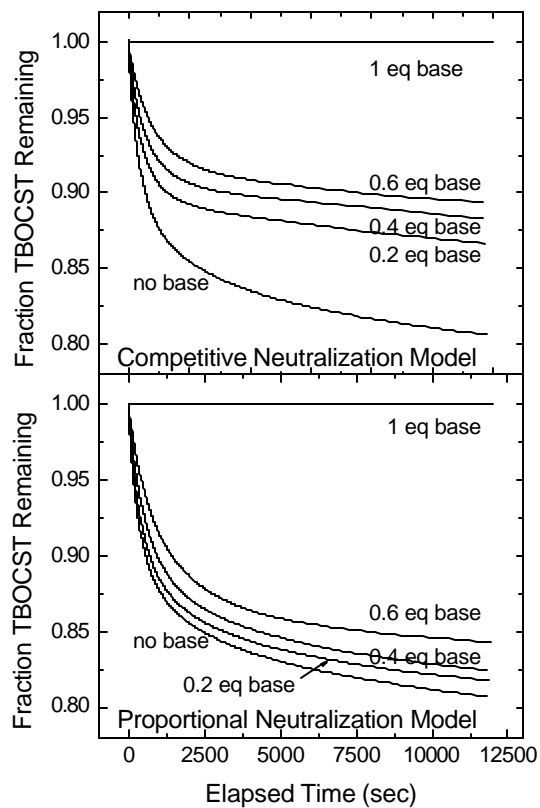


Figure 3 . Model predictions for the effect of added base on the extent of PTBOCST deprotection with time during post-exposure bake at 65 C.

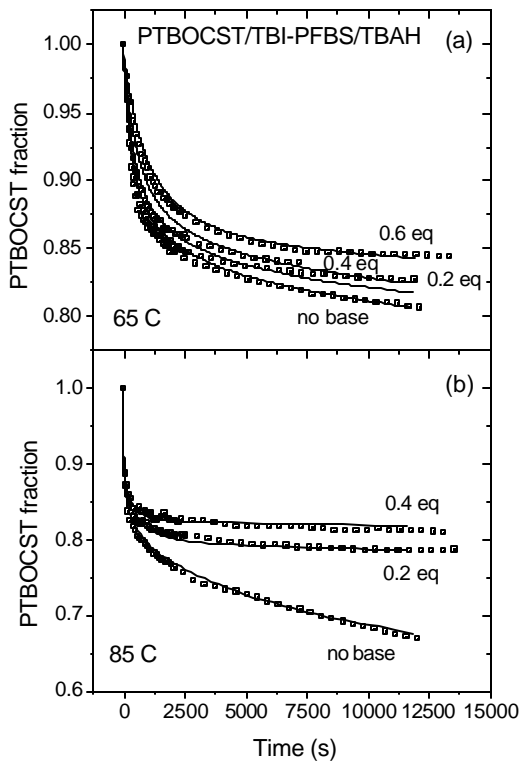


Figure 4 . Comparison of experimental results (points) measuring the effect on PTBOCST deprotection kinetics of adding various equivalencies of TBAH to simulations (lines) using the PN model: (a) post-exposure bake at 65 C, (b) post-exposure bake at 85 C.

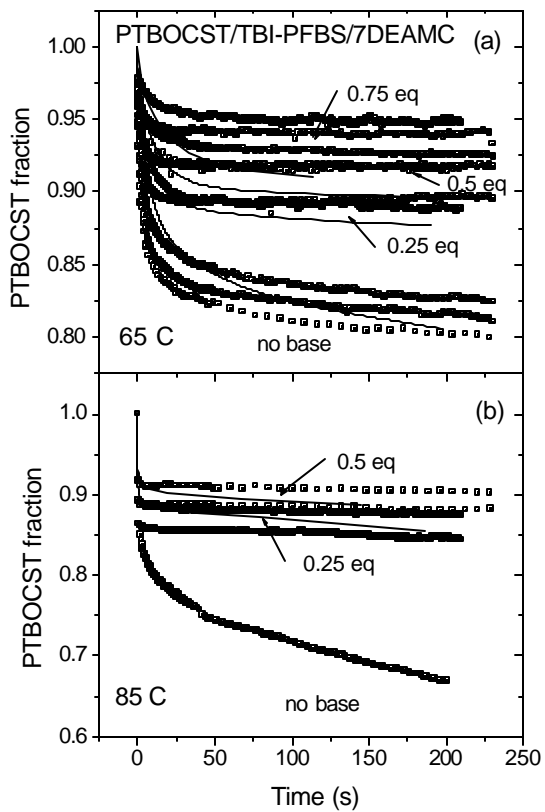


Figure 5. Comparison of experimental results (points) measuring the effect on PTBOCST deprotection kinetics of adding various equivalencies of 7DEAMC to simulations (lines) using the CN model: (a) post-exposure bake at 65 C, (b) post-exposure bake at 85 C.

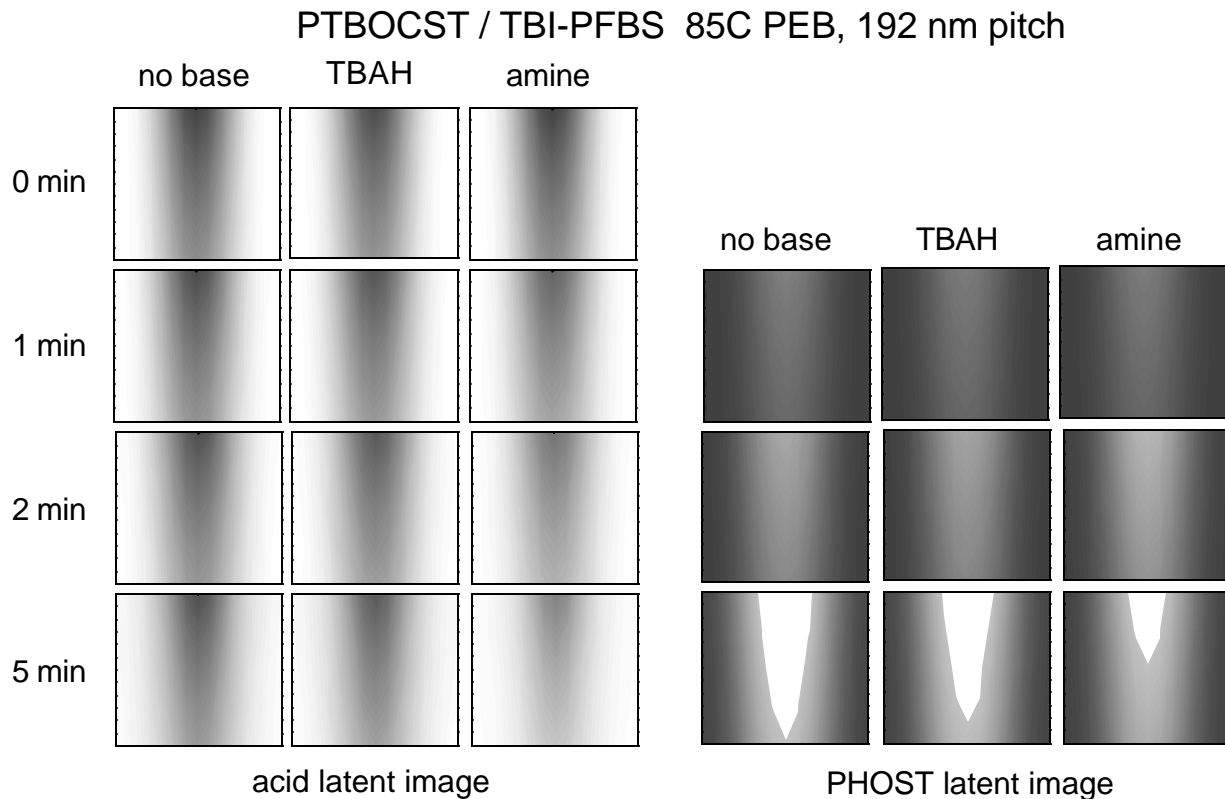


Figure 6. Maps of simulated acid and HOST latent images as they evolve during post-exposure bake at 85 C following an 8 mJ/cm² exposure (incident dose). Each map is for a single 192 nm period of an infinite line-space array. Images are compared for PTBOCST/TBI-PFBS resist with no base, with 0.05 eq TBAH added, and with 0.05 eq of amine added. The grey scale for the acid images ranges from 0 (white) to 1.8e-20 moles (black), and for the deprotected polymer image from a HOST fraction of 0 (black) to 0.8 (white). Above 0.8 the resist is completely soluble, so the white regions are approximate resist profiles.

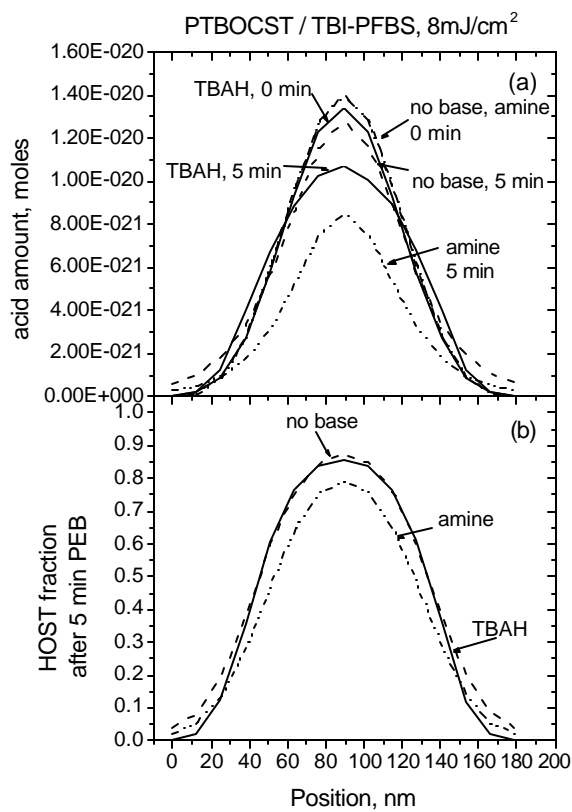


Figure 7. Comparison of simulated (a) average acid distributions at 0 and 5 min for the three formulations taken from the maps in Figure 6, and (b) deprotected PTBOCST profiles resulting from these distributions, 192 nm pitch, 8 mJ/cm² incident dose.

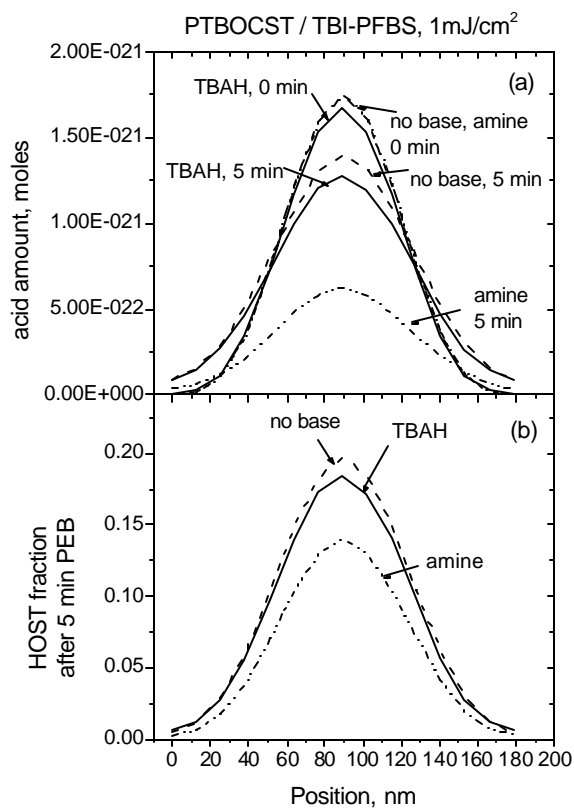


Figure 8. Comparison of simulated (a) average acid distributions at 0 and 5 min for the three resist formulations and (b) deprotected PTBOCST profiles resulting from these distributions, 192 nm pitch, 1 mJ/cm² incident dose. Maps are not shown

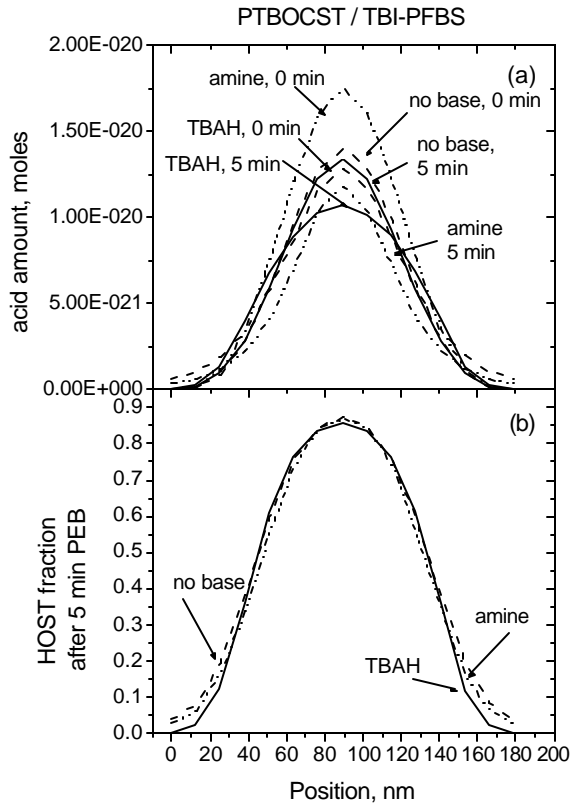


Figure 9. Comparison of simulated (a) average acid distributions at 0 and 5 min for the three resist formulations: amine at 10 mJ/cm² dose, and TBAH and no base at 8 mJ/cm² dose, and (b) deprotected PTBOCST profiles resulting from these distributions, 192 nm pitch. Maps are not shown. These simulations compare acid profiles that result in essentially identical deprotected resist images.

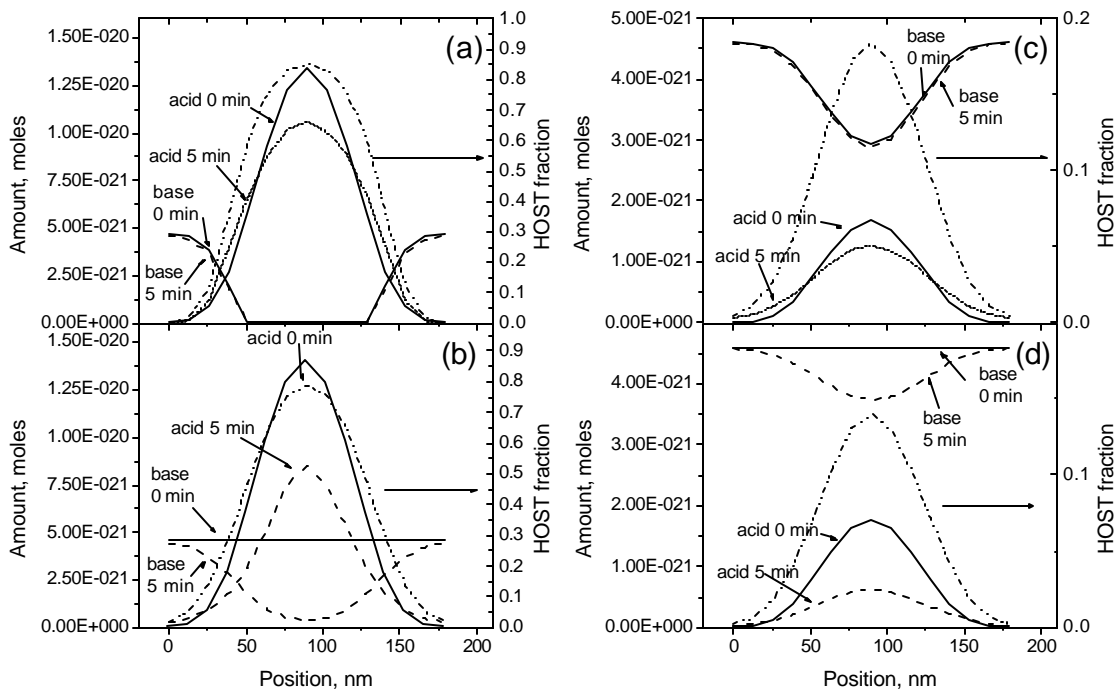


Figure 10. Simulated acid, base and deprotected PTBOCST (HOST) profiles at 0 and 5 min for the two PTBOCST/TBI-PFBS/base resist formulations, post-exposure bake temperature of 85C. (a) TBAH, 8 mJ/cm², (b) amine, 8 mJ/cm², (c) TBAH 1 mJ/cm², (d) amine, 1 mJ/cm². The profiles for the amine at 10 mJ/cm² are very similar to those at 8 mJ/cm², (b), and are not shown.

PTBOCST / TBI-PFBS 85C PEB, 500 nm pitch

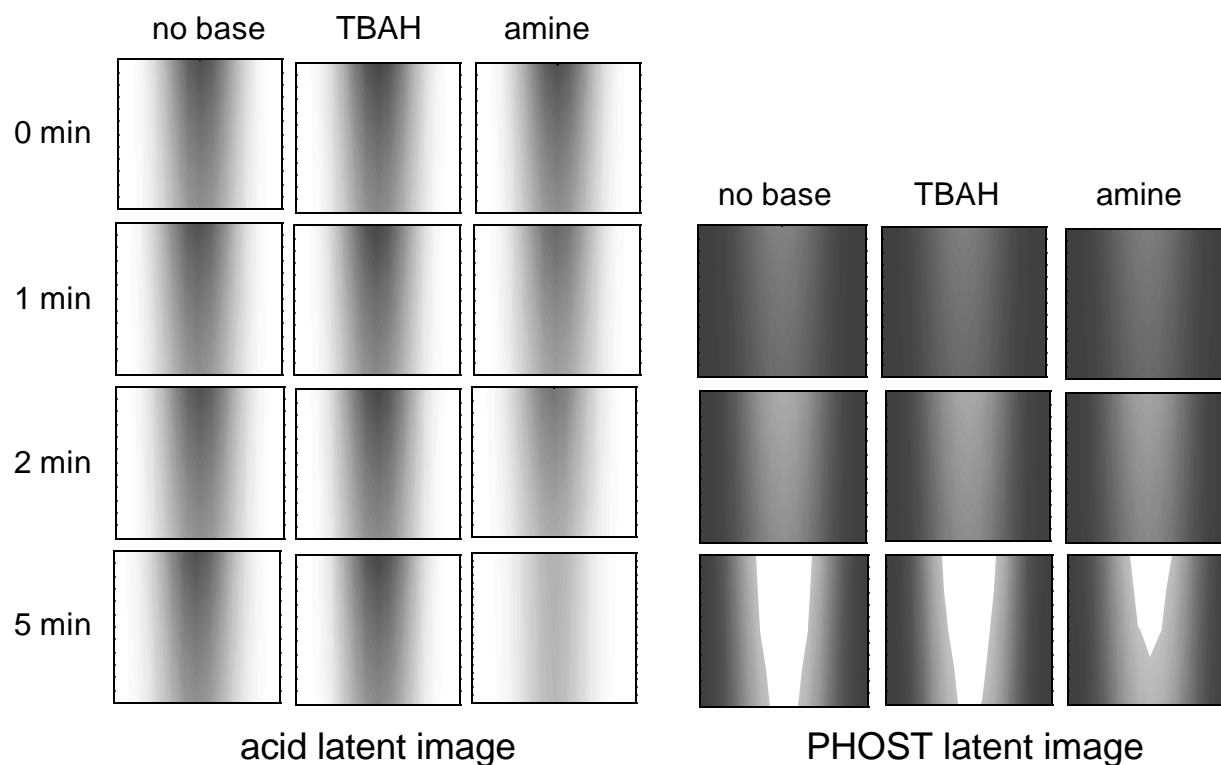


Figure 11. Maps of simulated acid and HOST latent images as they evolve during post-exposure bake at 85C following an 8 mJ/cm² exposure (incident dose). Each map is for a single 500 nm period of an infinite line-space array. Images are compared for PTBOCST/TBI-PFBS resist with no base, with 0.05 eq TBAH added, and with 0.05 eq of amine added. The grey scale for the acid images ranges from 0 (white) to 5e-20 moles (black), and for the deprotected polymer image from a HOST fraction of 0 (black) to 0.8 (white). Above 0.8 the resist is completely soluble, so the white regions are approximate resist profiles.

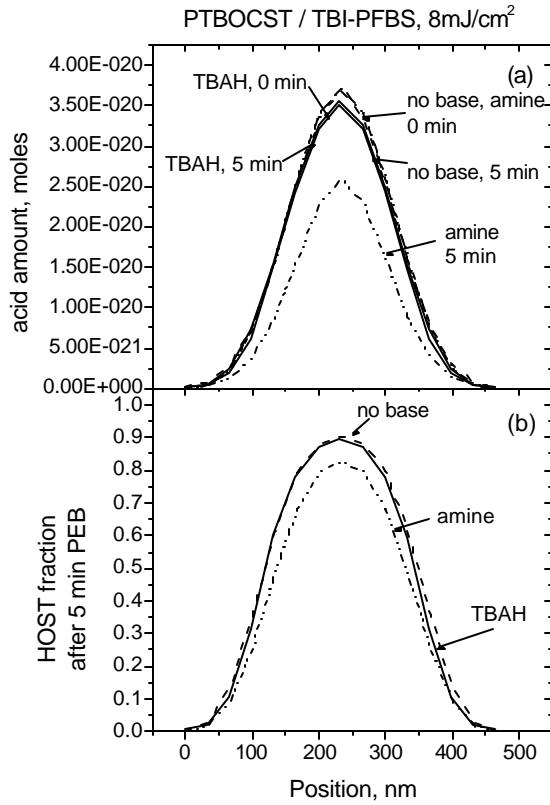


Figure 12. Comparison of simulated (a) average acid distributions at 0 and 5 min for the three resist formulations taken from the maps in Figure 10, and (b) deprotected PTBOCST profiles resulting from these distributions, 500 nm pitch, 8 mJ/cm² incident dose.

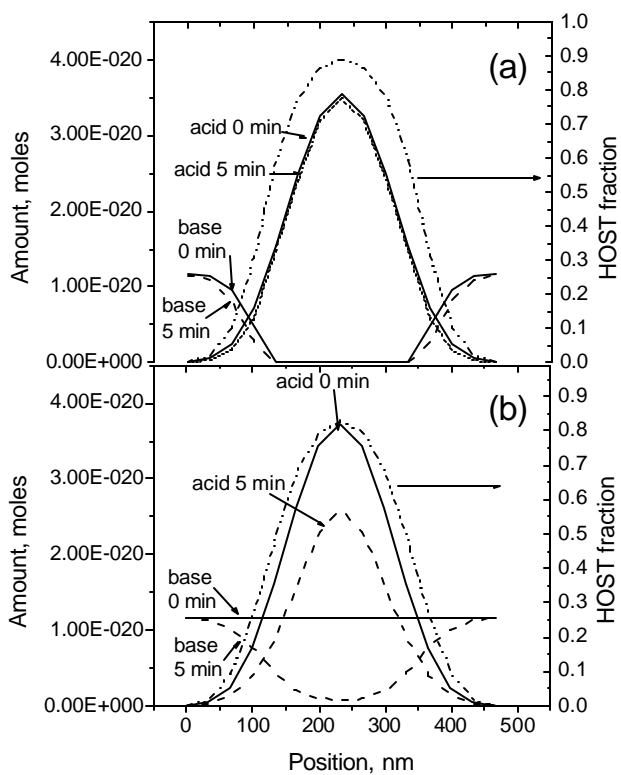


Figure 13. Simulated acid, base and deprotected PTBOCST (HOST) profiles at 0 and 5 min for the two PTBOCST/TBI-PFBS/base resist formulations, incident dose of 8 mJ/cm², post-exposure bake temperature of 85C. (a) TBAH, (b) amine.

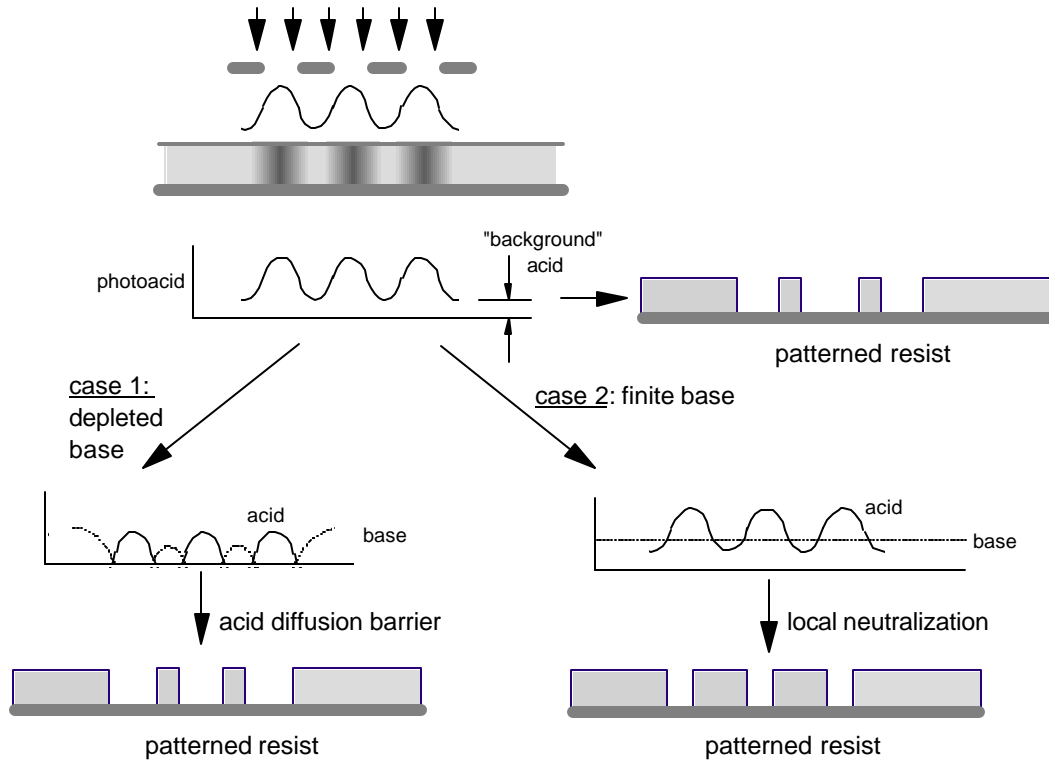


Figure 14. Schematic of the role of added base in resist imaging determined in this work. An exposure of a resist that contains no base results in formation of an acid latent image which can form a distorted pattern due to small amounts of acid in nominally unilluminated areas. If base is added two limiting cases can be distinguished. Case 1: base is depleted in highly acidic regions, and affects the resist image by serving as a diffusion barrier. Image blur is not necessarily reduced, but image contrast can be improved. Case 2: acid neutralization competes with deprotection, leading to reduction of image blur by reduction of local acid concentrations. Addition of base causes acid to be rapidly neutralized, leading to a more localized acid image.